

Evidence for extremely rapid magma ocean crystallization and crust formation on Mars

Bouvier Laura C. ^{1,2}, Costa Maria M. ^{1,2}, Connelly James N. ^{1,2}, Jensen Ninna K. ^{1,2}, Wielandt Daniel ^{2,3}, Storey Michael ^{2,3}, Nemchin Alexander A. ⁴, Whitehouse Martin J. ⁵, Snape Joshua F. ⁵, Bellucci Jeremy J. ⁵, Moynier Frederic ⁶, Agranier Arnaud ^{7,8}, Gueguen Bleuenn ^{7,8}, Schonbachler Maria ⁹, Bizzarro Martin ^{1,2,*}

¹ Univ Copenhagen, Ctr Star & Planet Format, Copenhagen, Denmark.

² Univ Copenhagen, Nat Hist Museum Denmark, Copenhagen, Denmark.

³ Univ Copenhagen, Quadlab, Copenhagen, Denmark.

⁴ Curtin Univ, Dept Appl Geol, Perth, WA, Australia.

⁵ Swedish Museum Nat Hist, Stockholm, Sweden.

⁶ Univ Paris Diderot, Sorbonne Paris Cite, Inst Phys Globe Paris, Paris, France.

⁷ Univ Bretagne Occidentale, CNRS, Lab Geosci Ocean, UMR 6538, Plouzane, France.

⁸ Inst Univ Europeen Mer, Plouzane, France.

⁹ ETH, Inst Geochem & Petr, Zurich, Switzerland.

* Corresponding author : Martin Bizzarro, email address : bizzarro@snm.ku.dk

Abstract :

The formation of a primordial crust is a critical step in the evolution of terrestrial planets but the timing of this process is poorly understood. The mineral zircon is a powerful tool for constraining crust formation because it can be accurately dated with the uranium-to-lead (U-Pb) isotopic decay system and is resistant to subsequent alteration. Moreover, given the high concentration of hafnium in zircon, the lutetium-to-hafnium (Lu-176-Hf-176) isotopic decay system can be used to determine the nature and formation timescale of its source reservoir(1-3). Ancient igneous zircons with crystallization ages of around 4,430 million years (Myr) have been reported in Martian meteorites that are believed to represent regolith breccias from the southern highlands of Mars(4,5). These zircons are present in evolved lithologies interpreted to reflect re-melted primary Martian crust(4), thereby potentially providing insight into early crustal evolution on Mars. Here, we report concomitant high-precision U-Pb ages and Hf-isotope compositions of ancient zircons from the NWA 7034 Martian regolith breccia. Seven zircons with mostly concordant U-Pb ages define Pb-207/Pb-206 dates ranging from 4,476.3 +/- 0.9 Myr ago to 4,429.7 +/- 1.0 Myr ago, including the oldest directly dated material from Mars. All zircons record unradiogenic initial Hf-isotope compositions inherited from an enriched, andesitic-like crust extracted from a primitive mantle no later than 4,547 Myr ago. Thus, a primordial crust existed on Mars by this time and survived for around 100 Myr before it was reworked, possibly by impacts(4,5), to produce magmas from which the zircons crystallized. Given that formation of a stable primordial crust is the end product of planetary differentiation, our data require that the accretion, core formation and magma ocean crystallization on Mars were completed less than 20 Myr after the formation of the Solar System. These timescales support models that suggest extremely rapid magma ocean crystallization leading to a gravitationally unstable stratified

mantle, which subsequently overturns, resulting in decompression melting of rising cumulates and production of a primordial basaltic to andesitic crust(6,7).

$^{207}\text{Pb}/^{206}\text{Pb}$ dates ranging from 4476.3 ± 0.9 Ma to 4429.7 ± 1.0 Ma, including the oldest directly dated material from Mars. All zircons record unradiogenic initial Hf-isotope compositions inherited from an enriched, andesitic-like crust extracted from a primitive mantle no later than 4547 Ma. Thus, a primordial crust existed on Mars by this time and survived for ~ 100 Myr before it was reworked, possibly by impacts^{4,5}, to produce magmas from which the zircons crystallized. Given that formation of a stable primordial crust is the end product of planetary differentiation, our data require that the accretion, core formation and magma ocean crystallization on Mars was completed < 20 Myr after Solar System formation. These timescales support models suggesting rapid magma ocean crystallization leading to a gravitationally unstable stratified mantle, which subsequently overturns resulting in decompression melting of rising cumulates and extraction of a primordial basaltic to andesitic crust^{6,7}.

The emergence of a stable primordial crust is a fundamental step in the early history of rocky, potentially habitable planets. Primordial crust formation is the end product of a long sequence of events, including planetary accretion, establishment of a global magma ocean, core formation and, finally, silicate differentiation. Existing constraints^{6–12} for the timing of each of these events allow for primordial crust formation in terrestrial planets over timescales of ~ 5 to ~ 100 Myr, a range that precludes a full understanding of early planet formation. In the Solar System, Mars offers a unique possibility to better constrain the timing of planet-formation processes given its relatively simple geologic history as a stranded planetary embryo⁸ as well as the wealth of information from martian meteorites and spacecraft exploration¹³. Based on the meteorite record, the accretion of Mars is inferred to have been largely completed within ~ 5 Myr of Solar System formation^{8,14} whereas the crystallization of the magma ocean leading to the extraction of a primordial crust may have occurred over timescales of ~ 30 to ~ 100 Myr after accretion^{10,15,16}. However, these timescales for silicate differentiation are based on the modelled abundances of the short-lived ^{182}Hf and ^{146}Sm nuclides during planetary differentiation inferred from young martian meteorites and, hence, highly model dependent.

A more robust approach to dating early planetary differentiation on Mars requires the identification of material that formed in the earliest evolutionary stages of the planet. On Earth, such a record is preserved in the Jack Hills of Western Australia that contains ancient zircons as old as ~ 4370 Ma¹⁷. Although zircon is not common in martian meteorites, two recent studies have reported the presence of ~ 4430 Ma zircons in the martian regolith breccia NWA 7533/7034 thought to have originated from the southern highlands of Mars^{4,5}. The breccia comprises clasts that are interpreted to be of igneous, sedimentary and impact origin, preserved in a fine-grained matrix. Zircons have been identified in the igneous and sedimentary clasts as well as within the matrix. Collectively, these grains are likely to provide the earliest tangible record of crust formation processes on Mars. However, the typical sizes of these zircons preclude obtaining concomitant U-Pb ages and Hf isotope compositions of sufficient precision using *in situ* techniques.

We conducted a systematic search for zircons from a bulk crushed rock aliquot of the NWA 7034 meteorite. Although this approach does not provide a petrological context for individual zircons, it is the only means of ensuring the recovery of grains sufficiently large

(>30 μm) for high-precision U-Pb chronology and Hf isotope measurements using solution-based methods. Irrespective of their petrological context, these zircons faithfully record information about the nature of their source reservoir. This rationale is recognized in studies using the Jack Hills detrital zircons to probe the early terrestrial crustal record¹⁷. A total of seven grains were extracted and analysed for U-Pb dating and Lu-Hf systematics. Their sizes ranged from ~50 to 110 μm and they were found to represent different morphologic types, including irregular anhedral pieces, euhedral with well-defined faces and a flat prismatic shape and, finally, rounded in shape (Extended Data Figure 1). Common to all of them was the general absence of fractures and inclusions, as well as any evidence for radiation damage. The zircons returned $^{207}\text{Pb}/^{206}\text{Pb}$ ages ranging from 4476.3 ± 0.9 Ma to 4429.7 ± 1.0 Ma (Table 1). Importantly, five out of the seven grains are concordant within their stated uncertainties, grain S22b5 is 1.2% discordant and grain S24B2 5.3% discordant (Fig. 1). The larger degree of discordance for grain S24B2 is consistent with its higher U content of 46 ppm relative to the other zircons we investigated. Based on textural information and geological context, the zircons from the basaltic breccia NWA 7034/7533 have been interpreted as igneous in origin^{4,5}. Both the ages and the morphologies of the zircons analysed here are in line with this interpretation. Although the range of ages we report is consistent with earlier studies, the better than ten-fold improvement in precision allows us to establish that zircon formation occurred in multiple igneous events over ~50 Myr. Four zircons analysed here define an age cluster at ~4475 Ma (Fig. 1), which is significantly older than the age of ~4430 Ma inferred from earlier studies of martian zircons. In particular, one concordant zircon (S25B10) from this population records an age of 4476.3 ± 0.9 Ma and, as such, represents the oldest directly dated material from Mars. This age is ~100 Myr older than the oldest dated terrestrial zircons¹⁷, implying that the record of crust forming processes on Mars is significantly older than that on Earth. Thus, these zircons provide a unique window into the earliest history of the planet.

The distinct geochemical behaviour of Lu and Hf during partial melting episodes makes the ^{176}Lu -to- ^{176}Hf decay system a powerful tool to constrain the timing of planetary silicate differentiation. For example, a primordial crustal reservoir will inherit a sub-chondritic $^{176}\text{Lu}/^{177}\text{Hf}$ ratio (<0.0336, ref. 18) such that its time-integrated Hf isotopic composition will be less radiogenic than the chondritic uniform reservoir (CHUR). We have determined the Hf isotope composition and Lu/Hf ratios of the seven U-Pb dated zircons using multiple collection inductively coupled plasma source mass spectrometry (MC-ICPMS)^{19,20}. The more than four-fold improvement in precision afforded by this method over *in situ* techniques (e.g. ref. 21) is required to probe early differentiation timescales given the small amount radiogenic ingrowth of ^{176}Hf in the first 100 Myr of the Solar System. Moreover, this approach guarantees that the Hf isotope compositions were measured on the same volume of zircon for which the ages were determined, thereby ensuring that the initial Hf isotope compositions are accurately time-corrected. Importantly, the age variability of ~50 Myr recorded by the zircons allow us to track the isotopic evolution of their source reservoir. The seven zircons have unradiogenic initial ϵHf values ranging from -0.71 ± 0.32 to -2.06 ± 0.26 (Table 1; the ϵHf value is the deviation of the $^{176}\text{Hf}/^{177}\text{Hf}$ ratio of a sample from the chondritic uniform reservoir, CHUR, in parts per 10^4), indicating that these grains formed from a precursor reservoir with a sub-chondritic $^{176}\text{Lu}/^{177}\text{Hf}$ ratio (Fig. 2a). The

initial ϵHf value are correlated with their $^{207}\text{Pb}/^{206}\text{Pb}$ ages, suggesting that these grains were ultimately derived from a common source reservoir. The stable $^{178}\text{Hf}/^{177}\text{Hf}$ and $^{180}\text{Hf}/^{177}\text{Hf}$ ratios of the NWA 7034 zircons are identical to terrestrial zircons (Table 1), establishing that the reported ϵHf values are unaffected by neutron capture effects.

The minimum model formation age for the source reservoir of the zircon population investigated here can be estimated from the oldest grain that record the most unradiogenic initial Hf isotope composition. Three of the four zircons that define the age cluster at ~ 4475 Ma have concordant U-Pb ages and, as such, inferred to have undisturbed ^{176}Lu - ^{176}Hf systematics. Indeed, these three zircons (S24b4, S24b7 and S25b10) record identical initial ϵHf values within uncertainty despite different $^{176}\text{Lu}/^{177}\text{Hf}$ ratios. Thus, the average initial ϵHf value of these three concordant grains (-1.35 ± 0.22) provides a robust estimate of the Hf isotope composition of their protolith at ~ 4475 Ma and, hence, the formation age of their source crustal reservoir. Given that the available geochemical data suggest that the bulk of the exposed martian crust is of basaltic composition^{13,22}, we assess whether this type of crust could represent the source reservoir of the ancient zircon population. Using a $^{176}\text{Lu}/^{177}\text{Hf}$ ratio typical of mafic crustal sources on Earth (0.020, ref. 23) returns impossibly old ages (>4567 Ma), requiring the existence of a crustal reservoir with a composition more evolved than basaltic to account for the initial ϵHf value of the ~ 4475 Ma zircons. A possibility is an andesite-like source, as rocks with such evolved compositions have been identified on Mars based on *in situ* observations²⁴. Moreover, some magma ocean crystallization models^{6,7} predict basaltic to andesitic compositions for the primary martian crust produced by decompression melting of rising cumulates, following overturn of the gravitationally unstable stratified mantle. We note that recent estimates that suggest a low crustal bulk density for Mars (2582 ± 209 kg/m³, ref. 25) could, in principle, also be consistent with a more evolved average crustal composition. Using an andesite-like $^{176}\text{Lu}/^{177}\text{Hf}$ ratio of ~ 0.011 estimated from terrestrial rocks^{23,26} defines a minimum formation age of 4547 Ma for the source reservoir. An andesite-like composition for the nature of this source reservoir is further reinforced by the observation that the initial Hf isotope compositions of the ~ 4450 Ma and ~ 4430 Ma zircons are also consistent with extraction from the same source (Fig. 2b). Indeed, taking the data at face value for each of the age groups returns a slope corresponding to an andesite-like $^{176}\text{Lu}/^{177}\text{Hf}$ ratio of ~ 0.011 . The fact that more evolved compositions for a primordial crust are not predicted by any model provides confidence that the formation age of this reservoir cannot be younger than 4547 Ma. Therefore, this minimum age for the source of the NWA 7034 zircons represents the oldest differentiated silicate reservoir yet identified on Mars. Ancient martian zircons with ages comparable to that reported here have been identified in igneous, evolved lithologies that are interpreted to reflect re-melted primary martian crust⁴. The enriched composition for the NWA 7034 zircon source reservoir inferred from the andesite-like $^{176}\text{Lu}/^{177}\text{Hf}$ ratio is consistent with this interpretation. Thus, our new data require that a primordial crust existed on Mars by 4547 Ma and that it survived for ~ 100 Myr before it was reworked to produce magmas, possibly by impacts^{4,5}, from which the NWA 7034 zircons crystallized. We infer that this primordial crust represents a global reservoir given its longevity and the extended period of reworking indicated by the zircon data.

The new timescales reported here for stabilization of the primordial martian crust have far reaching implications for understanding the accretion and differentiation history of Mars. Given that the formation of a stable primordial crust is the end product of the initial planetary differentiation, our data require that accretion, core formation and magma ocean crystallization on Mars was completed within 20 Myr of Solar System formation. Such short timescales for primary accretion are predicted by planet formation models invoking pebble accretion where growth is fuelled by the gas-drag assisted accretion of mm-sized objects, which leads to the efficient formation of Mars-sized embryos within the ~5 Myr lifetime of the protoplanetary disk^{27,28}. Moreover, these timescales are also consistent with estimates based on the short-lived ^{182}Hf - ^{182}W decay system for the timing of core formation, which is inferred to have occurred within 10 Myr of Solar System formation²⁹. In contrast, some recent studies have suggested that magma ocean crystallization was protracted on Mars, perhaps lasting up to ~100 Myr, based on model ages deduced from the abundances of short-lived radionuclides in young martian meteorites^{10,15,16}. Such a protracted magma ocean crystallization is inconsistent with the data presented here and thermal models suggesting that the solidification history of Mars must have been completed within ~10 Myr of accretion⁷. As such, the timing of silicate differentiation inferred from short-lived radionuclides in young martian meteorites may not reflect primary differentiation of the planet but rather a younger, mantle-scale, fractionation event. Finally, our data and interpretation are fully consistent with models suggesting rapid magma ocean crystallization leading to a gravitationally unstable stratified mantle, which subsequently overturns resulting in decompression melting of rising cumulates and extraction of a primordial basaltic to andesitic crust^{6,7}. The extensive resurfacing of Mars by volcanism over the planet's history predicts that if any primordial crust is preserved, it will reside at depth and may only be exposed in deep craters.

Methods

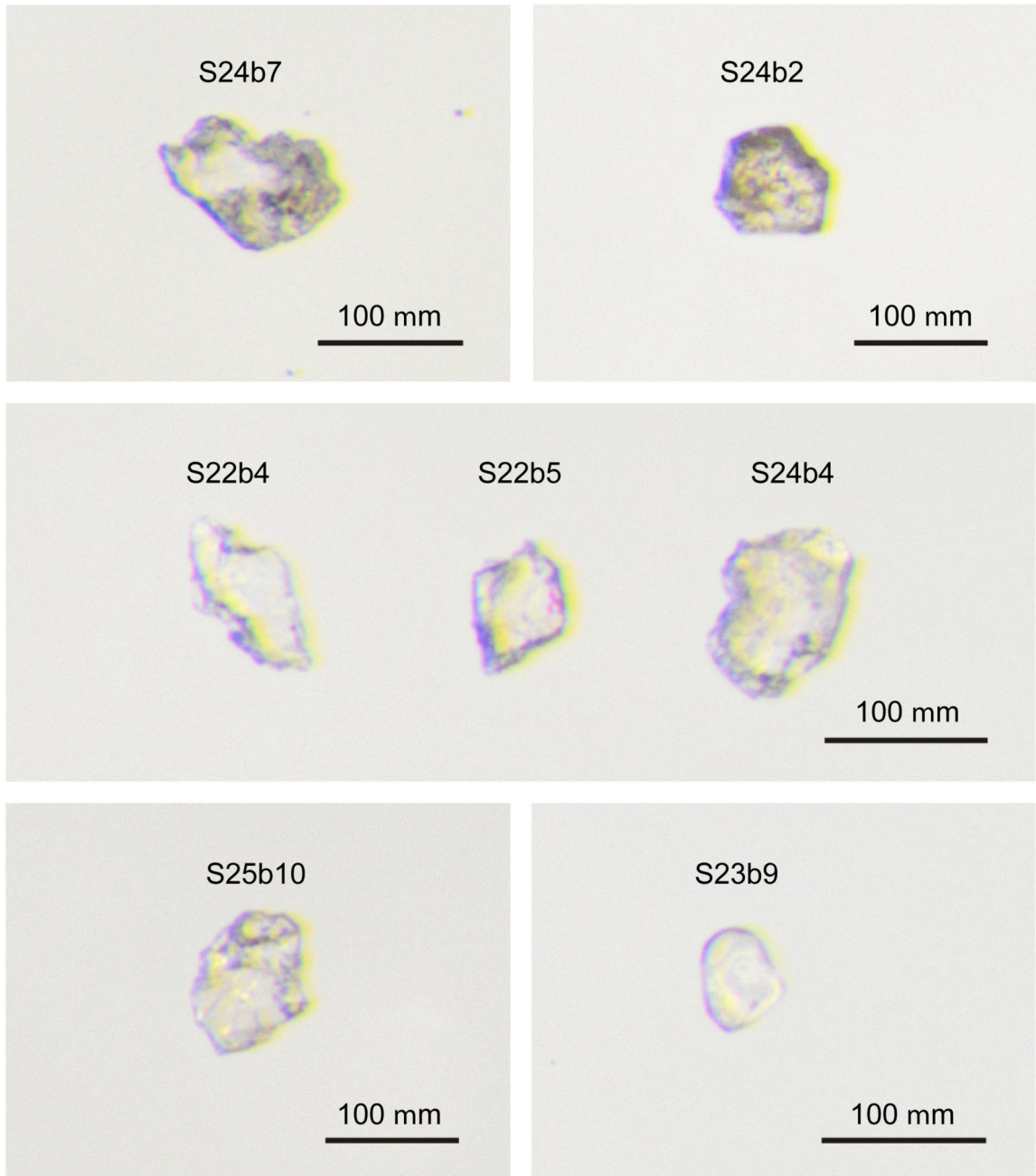
A total of seven zircon grains were extracted from a crushed bulk rock aliquot of NWA 7034 and analysed for U-Pb and Lu-Hf systematics. Given the limited number of zircons recovered from the crushing process and their small sizes, only one of the larger grains (S25b10) was chemically abraded³². This pre-treatment consisted of thermally annealing the less metamict domains of the crystal over three days at 900°C, followed by dissolution of the un-annealed portions using concentrated HF for 12 h at 180°C in Teflon capsules. Before complete dissolution, all zircon grains were cleaned in pyrex beakers in an ultrasonic bath with alternating steps of warm 3.5 M HNO₃, H₂O and acetone. Assuming that each grain may represent a different age, they were processed as single-grains. The individual crystals were dissolved in separate PFE Teflon capsules in an HF-HNO₃ (3:1) mixture, together with the mixed ^{202}Pb - ^{205}Pb - ^{233}U - ^{235}U EARTHTIME U-Pb tracer³³, for four days at 210°C. The dissolved samples were evaporated to dryness and redissolved in 3.1M HCl overnight. Uranium and lead were separated from the matrix elements by anion chromatography using 50 µl Teflon columns^{34,35} and dried down together with 8 µl of 0.1 M H₃PO₄. They were loaded with silica gel³⁶ on previously-outgassed zone-refined Re filaments. The Pb and U isotopic ratios of the sample-tracer mixture were measured using the Triton Thermo-Fisher thermal ionization mass spectrometer at the Centre for Star and Planet Formation, University

of Copenhagen, where each isotope was sequentially counted in a single axial ion counting system with Pb as Pb^+ , and U as UO^{2+} . The data were reduced offline and instrumental mass fractionation was accounted for by a linear mass-dependent fractionation law based on the $^{202}\text{Pb}/^{205}\text{Pb}$ ratio of the tracer. After 1 pg of laboratory Pb blank was removed from the analyses, the remainder of common Pb was assumed to have an isotopic composition modelled after Bellucci *et al.*³⁷. Instrumental mass-dependent fractionation of U was accounted for using the $^{233}\text{U}/^{235}\text{U}$ ratio of the tracer, which included a correction for the isobaric interference of $^{233}\text{U}^{16}\text{O}^{18}\text{O}$ on the $^{235}\text{U}^{16}\text{O}_2$ peak at mass 267. The $^{238}\text{U}/^{235}\text{U}$ ratio of 137.88 (ref. 38) and the ^{238}U and ^{235}U decay constants of Jaffey *et al.*³⁹ were used for calculation of U/Pb ratios and ages. All ratios and age uncertainties are quoted at the 95% confidence level.

The Hf isotope composition and Lu/Hf ratios of individual zircons were determined from the same sample digestion used for U-Pb age determination. Following collection of the high field strength elements (HFSE) and rare earth elements (REE) washes from the U-Pb purification, approximately 5% of the solution was aliquoted for Lu/Hf ratio determination. The Hf was purified from the remaining solution by a two-step procedure using TEVA-spec and TODGA resins (Eichrom Industries) based on protocols outlined in Bizzarro *et al.*¹⁹ and in Connelly *et al.*²⁰. Zr was quantitatively separated from Hf, Ti and REE using 100-150 μm TEVA-spec resin in 120 μL column. The HFSE-REE fractions were loaded in 0.6 mL of 10.5M HCl and a Hf+Ti+REE cut was successively collected with 3.6mL of 10.5M HCl and 4.2 mL of 9.5M HCl. Zr was recovered with 3,0 mL of 6M HCl. Hf was purified from Ti and REE using 50-100 μm TODGA resin in 200 μL columns. The Hf+Ti+REE fractions were loaded in 0.85mL of 3.5M HNO_3 -0.06M boric acid and the Ti was eluted by adding 3.5 mL of 3.5M HNO_3 while Hf and REE remained on the column. Hf was subsequently collected with 6 mL of 1M HNO_3 -0.35M HF. This method returns Hf yields greater than 95% in Hf cuts with Zr/Hf ratios below 1. Hf isotope ratios were measured on the *Pandora* Thermo-Fisher Neptune Plus Multi-Collector Inductively Coupled Mass Spectrometer (MC-ICPMS) at the Centre for Star and Planet Formation, University of Copenhagen, using a sample-standard bracketing technique. Samples were aspirated into the plasma source in 2% HNO_3 -0.1M HF solution via a Cetac Aridus II desolvating nebulizer using Ar and N sweep gases with an uptake rate of $\sim 100 \mu\text{l}/\text{min}$. Typical sensitivity at this uptake rate was 1800V per ppm for Hf. Hafnium isotopic data were acquired in static mode using eight Faraday collectors allowing for simultaneous measurement of ^{176}Hf , ^{177}Hf , ^{178}Hf , ^{179}Hf and ^{180}Hf as well as monitoring potential isobaric interferences (^{176}Yb on ^{176}Hf , ^{176}Lu on ^{176}Hf and ^{180}W on ^{180}Hf) using ^{175}Lu , ^{171}Yb and ^{182}W . Faraday detectors used to collect Hf isotopes and ^{182}W were connected to amplifiers with 10^{11} Ohm feedback resistors whereas ^{175}Lu and ^{171}Yb were measured on Faraday detectors connected to amplifiers with 10^{13} Ohm feedback resistors. Sample analyses were interspersed with analyses of the JMC-475 standard as follows: JMC-475 (1), JMC-475 (2), sample-1, JMC-475 (3), JMC-475 (4). Samples and standards were analyzed with a signal intensity of at least 1V on mass ^{177}Hf and ensuring that the signal intensity of the sample and standard were matched to within 5%. Samples were analyzed once and the total amount of Hf consumed per analysis was typically 2-5 ng for NWA 7034 zircons. Total procedural blanks were <10 pg for Hf, an amount that is negligible for all samples considering the amount of Hf available for analysis. All data

reduction was conducted offline using the freely available Iolite data reduction software⁴⁰ that runs within Igor Pro. Background intensities were interpolated using a smoothed cubic spline, as were changes in mass bias with time. Hf isotope data were corrected for mass bias using the exponential mass fractionation law adopting $^{179}\text{Hf}/^{177}\text{Hf} = 0.7325$. The sample $^{176}\text{Hf}/^{177}\text{Hf}$, $^{178}\text{Hf}/^{177}\text{Hf}$, $^{180}\text{Hf}/^{177}\text{Hf}$ ratios were normalised to the JMC-475 reference values of 0.282160, 1.46717 and 1.88667, respectively. Contribution from interfering species were on average 33 and 1 ppm on $^{176}\text{Hf}/^{177}\text{Hf}$ from Yb and Lu, respectively, and 26 ppm on $^{180}\text{Hf}/^{177}\text{Hf}$ from W. Doping experiments with Yb interference levels at least 10 times greater than typically observed in our sample demonstrate that our interference correction is accurate. The accuracy and external reproducibility of our method was assessed by repeat analyses of the 91500 zircon reference standard⁴¹. In detail, seven aliquots of the same sample dissolution each containing approximately 5 ng of Hf were individually processed through our U-Pb and Hf purification scheme and analysed following the methods described above. The average values obtained for the $^{176}\text{Hf}/^{177}\text{Hf}$, $^{178}\text{Hf}/^{177}\text{Hf}$, $^{180}\text{Hf}/^{177}\text{Hf}$ ratios of the 91500 standard aliquots were 0.282311 ± 0.000006 , 1.46718 ± 0.00002 and 1.88669 ± 0.00006 , where the uncertainty represents the external reproducibility (2SD) (Table 1). The data we obtained for the 91500 zircon reference standard are identical to published values⁴².

The Lu/Hf ratios were determined by the same MC-ICPMS as used for the Hf isotopic measurements using gravimetrically prepared mixed Lu-Hf standard solutions. In detail, the ~5% aliquot reserved for Lu/Hf ratio determination was evaporated and re-dissolved in 2% HNO_3 -0.1M HF prior to analysis. Samples were aspirated into the plasma source via a Cetac Aridus II desolvating nebulizer using Ar and N sweep gases with an uptake rate of ~100 $\mu\text{L}/\text{min}$. The ^{175}Lu beam was collected on the axial secondary electron multiplier (SEM) whereas the ^{177}Hf was collected on the H2 faraday detector connected to an amplifier with a 10^{11} Ohm feedback resistor. Sample analyses were interspaced by analyses of the calibrated Lu-Hf standard solution as follows: Lu-Hf standard (1), Lu-Hf standard (2), sample-1, Lu-Hf standard (3), Lu-Hf standard (4). Samples and standard were analyzed with an intensity at least ~0.05 V on mass ^{177}Hf and ~100.000 cps on mass ^{175}Lu , ensuring that the signal intensity of the sample and standard were matched to within ~5%. Total procedural blanks were <5 fg for Lu and negligible for all samples considering the amount of Lu available for analysis. The Lu-Hf standard solution was prepared gravimetrically to match the typical Lu/Hf ratio of zircon and is accurate to 2%. The external reproducibility of our approach was estimated by repeated analysis of the 91500 zircon standard. Analysis of 10 individual aliquots of a single dissolution of the 91500 zircon standard yielded a $^{176}\text{Lu}/^{177}\text{Hf}$ ratio of 0.00030346 ± 0.0000016 (2SD), which corresponds to an external reproducibility of 0.5% for the Lu/Hf ratio. Potential fractionation of the Lu/Hf ratio induced by U-Pb purification was evaluated by measuring the Lu/Hf ratios of aliquots of the 91500 zircon standard before and after U-Pb purification. Our tests demonstrate that potential fractionation of the Lu/Hf during U-Pb purification is less than 0.4%. Combined with the uncertainty of the Lu-Hf standard solution, the external reproducibility of 0.5% and the potential fractionation of 0.4%, we infer an accuracy of 2.1% for our Lu/Hf ratio measurements. This represents the total uncertainty on the Lu/Hf ratio reported here and has been propagated in the final uncertainties quoted for the initial Hf isotope composition of the NWA 7034 zircons.

Extended Data**Extended Data Figure 1.**

Photomicrographs of the NWA 7034 zircons analysed in this study taken under natural light. Given the limited number of zircons recovered from the crushing process and their small sizes, it was deemed preferable not to conduct additional imaging (i.e. cathodoluminescence) as this necessitate extra manipulation of the individual grains thereby increasing the risk of losing zircons. The fact that the zircons have mostly concordant U-Pb

ages confirms their simple igneous history and, therefore, additional imaging to investigate potential zoning is not required here.

Supplementary Material

Refer to Web version on PubMed Central for supplementary material.

Acknowledgments

Financial support for this project was provided by the Danish National Research Foundation (DNRF97) and the European Research Council (ERC Consolidator Grant Agreement 616027 — STARDUST2ASTEROIDS) to M.B. We thank Jens Frydenvang and Kjartan Kinch for discussion.

References

1. Stevenson RK, Patchett PJ. Implications for the evolution of continental-crust from Hf-isotope systematics of Archean detrital zircons. *Geochim Cosmochim Acta*. 1990; 54:1683–1697.
2. Amelin Y, Lee D-C, Halliday AN, Pidgeon RT. Nature of the Earth's earliest crust from hafnium isotopes in single detrital zircons. *Nature*. 1999; 399:252–255.
3. Amelin Y, Lee D-C, Halliday AN. Early-middle Archean crustal evolution deduced from Lu-Hf and U-Pb isotopic studies of single grain zircons. *Geochim Cosmochim Acta*. 2000; 64:4205–4225.
4. Humayun M, et al. Origin and age of the earliest Martian crust from meteorite NWA 7533. *Nature*. 2013; 503:513–516. [PubMed: 24256724]
5. McCubbin FM, et al. Geologic history of Martian regolith breccia Northwest Africa 7034: Evidence for hydrothermal activity and lithologic diversity in the Martian crust. *Journal of Geophysical Research: Planets*. 2016; 121:2120–2149.
6. Elkins-Tanton LT, Hess PC, Parmentier EM. Possible formation of ancient crust on Mars through magma ocean processes. *Journal of Geophysical Research: Planets*. 2005; 110 E12S01.
7. Elkins-Tanton LT. Linked magma ocean solidification and atmospheric growth for Earth and Mars. *Earth and Planetary Science Letters*. 2008; 271:181–191.
8. Dauphas N, Pourmand A. Hf–W–Th evidence for rapid growth of Mars and its status as a planetary embryo. *Nature*. 2011; 473:489–492. [PubMed: 21614076]
9. Nimmo F, Tanaka K. Early crustal evolution of Mars. *Annual Review of Earth and Planetary Sciences*. 2005; 33:133–161.
10. Borg LE, Brennecka GA, Symes SJK. Accretion timescale and impact history of Mars deduced from the isotopic systematics of martian meteorites. *Geochimica et Cosmochimica Acta*. 2016; 175:150–167.
11. Caro G. Early silicate Earth differentiation. *Annual Review of Earth and Planetary Sciences*. 2011; 39:31–58.
12. Carlson RW, et al. How did early Earth become our modern world? *Annual Review of Earth and Planetary Sciences*. 2014; 42:151–178.
13. McSween HY. Petrology on Mars. *American Mineralogist*. 2015; 100:2380–2395.
14. Schiller M, Bizzarro M, Fernandes VA. Isotopic evolution of the protoplanetary disk and the building blocks of Earth and Moon. *Nature*. 2018 in press.
15. Debaille V, Brandon AD, Yin Q-Z, Jacobsen B. Coupled ^{142}Nd - ^{143}Nd evidence for protracted magma ocean in Mars. *Nature*. 2007; 450:525–528. [PubMed: 18033291]
16. Kruijer TS, et al. The early differentiation of Mars inferred from Hf-W chronometry. *Earth and Planetary Science Letters*. 2017; 474:345–354.
17. Whitehouse MJ, Nemchin AA, Pidgeon RT. What can Hadean detrital zircon really tell us? A critical evaluation of their geochronology with implications for the interpretation of oxygen and hafnium isotopes. *Gondwana Research*. 2017; 51:78–91.

18. Bouvier A, Vervoort JD, Patchett PJ. The Lu–Hf and Sm–Nd isotopic composition of CHUR: Constraints from unequilibrated chondrites and implications for the bulk composition of terrestrial planets. *Earth and Planetary Science Letters*. 2008; 273:48–57.
19. Bizzarro M, Baker JA, Ulfbeck D. A new digestion and chemical separation technique for rapid and highly reproducible of Lu/Hf and Hf isotope ratio in geological material by MC-ICP-MS. *Geostandard Newsletters*. 2003; 27:133–145.
20. Connelly JN, Ulfbeck DG, Thrane K, Bizzarro M, Housh T. A method for purifying Lu and Hf for analysis by MC-ICP-MS using TODGA resin. *Chemical Geology*. 2006; 233:126–136.
21. Kemp AIS, et al. Hadean crustal evolution revisited: New constraints from Pb–Hf isotope systematics of the Jack Hills zircons. *Earth and Planetary Science Letters*. 2010; 296:45–56.
22. McSween HY, Taylor J, Wyatt MB. Elemental Composition of the Martian Crust. *Science*. 2009; 324:736–739. [PubMed: 19423810]
23. Rudnick RL, Gao S. Composition of the continental crust. *The Crust, Treatise on Geochemistry*. Rudnick RL, editor. Vol. 3. Elsevier; Amsterdam: 2003. 1–64.
24. Sautter V, et al. In situ evidence for continental crust on early Mars. *Nature Geoscience*. 2015; 8:605–609.
25. Goossens S, Sabaka TJ, Genova A, Mazarico E, Nicholas JB, Neumann GA. Evidence for a Low Bulk Crustal Density for Mars from Gravity and Topography. *Geophysical Research Letters*. 2017; 44:7686–7694. [PubMed: 28966411]
26. Condie KC. Chemical composition and evolution of the upper continental crust: Contrasting results from surface samples and shales. *Chemical Geology*. 1993; 104:1–37.
27. Johansen A, Mac Low MM, Lacerda P, Bizzarro M. Growth of asteroids, planetary embryos, and Kuiper belt objects by chondrule accretion. *Sci Adv*. 2015; 1 e1500109.
28. Bollard J, et al. Early formation of planetary building blocks inferred from Pb isotopic ages of chondrules. *Sci Adv*. 2017; 3 e1700407.
29. Mezger K, Debaille V, Kleine T. Core formation and mantle differentiation on Mars. *Space Science Review*. 2013; 174:27–48.
30. Söderlund U, Patchett PJ, Vervoort JD, Isachsen CE. The ^{176}Lu decay constant determined by Lu–Hf and U–Pb isotope systematics of Precambrian mafic intrusions. *Earth and Planetary Science Letters*. 2004; 219:311–324.
31. Connelly JN, et al. The absolute chronology and thermal processing of solids in the solar protoplanetary disk. *Science*. 2012; 338:651–655. [PubMed: 23118187]
32. Mattinson JM, et al. Zircon U–Pb chemical abrasion ("CA-TIMS") method: Combined annealing and multi-step partial dissolution analysis for improved precision and accuracy of zircon ages. *Chemical Geology*. 2005; 220:47–66.
33. Condon DJ, Schoene B, McLean NM, Bowring SA, Parrish RR. Metrology and traceability of U–Pb isotope dilution geochronology (EARTHTIME Tracer Calibration Part I). *Geochimica et Cosmochimica Acta*. 2015; 164:464–480.
34. Krogh TE. A low contamination method for hydrothermal decomposition of zircon and extraction of U and Pb for isotopic age determination. *Geochimica et Cosmochimica Acta*. 1973; 37:485–494.
35. Corfu F. U–Pb age, setting and tectonic significance of the anorthosite–mangerite–charnockite–granite suite, Lofoten–Vesterålen, Norway. *Journal of Petrology*. 2004; 56:2081–2097.
36. Gerstenberger H, Haase G. A highly effective emitter substance for mass spectrometric Pb isotope ratio determinations. *Chemical Geology*. 1997; 136:309–312.
37. Bellucci JJ, et al. Pb-isotopic evidence for an early, enriched crust on Mars. *Earth and Planetary Science Letters*. 2015; 410:34–41.
38. Steiger RH, Jäger E. Subcommittee on geochronology: Convention on the use of decay constants in geo- and cosmochronology. *Earth and Planetary Science Letters*. 1977; 36:359–362.
39. Jaffey AH, Flynn KF, Glendenin LE, Bentley WC, Essling AM. Precision measurement of half-lives and specific of ^{235}U and ^{238}U . *Phys Rev*. 1971; C4:1889–1906.
40. Paton C, Hellstrom J, Paul B, Woodhead J, Hergt J. Iolite: freeware for the visualisation and processing of mass spectrometric data. *J Anal At Spectrom*. 2011; 26:2508–2518.

41. Wiedenbeck M, Allé P, Corfu F, Griffin WL, Meier M, Oberli F, von Quadt A, Roddick JC, Spiegel W. Three natural zircon standards for U-Th-Pb, Lu-Hf, trace element and REE analyses. *Geostandards Newsletter*. 1995; 19:1–23.
42. Blichert-Toft J. Hf isotopic composition of zircon reference material 91500. *Chemical Geology*. 2008; 253:252–257.

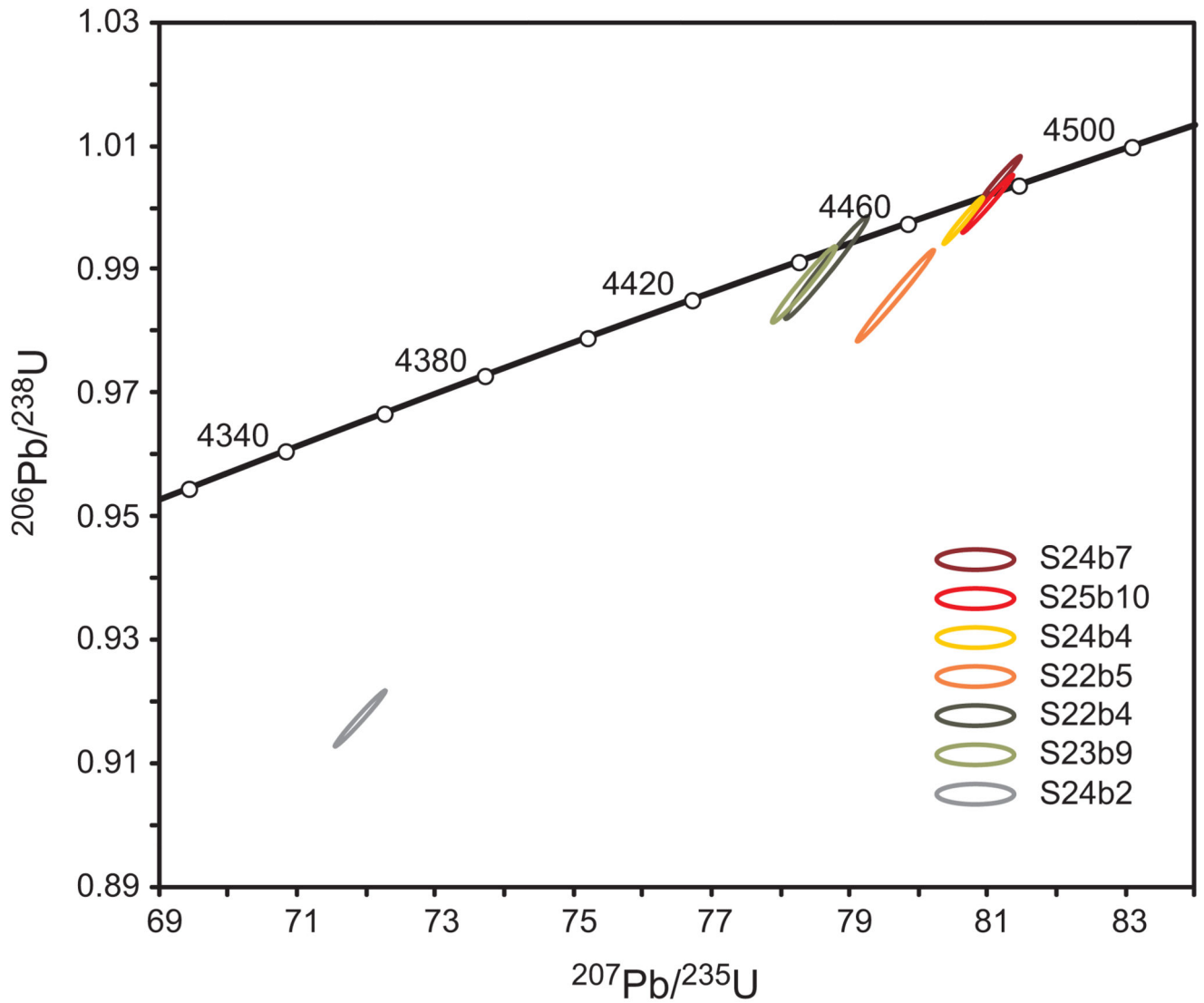


Fig. 1. U-Pb concordia diagram for seven zircon grains from the NWA 7034 meteorite.

Labels on concordia curve represent time before present in millions of years. Data-point error ellipses are 2σ . Data used in this figure are reported in full in Table S1.

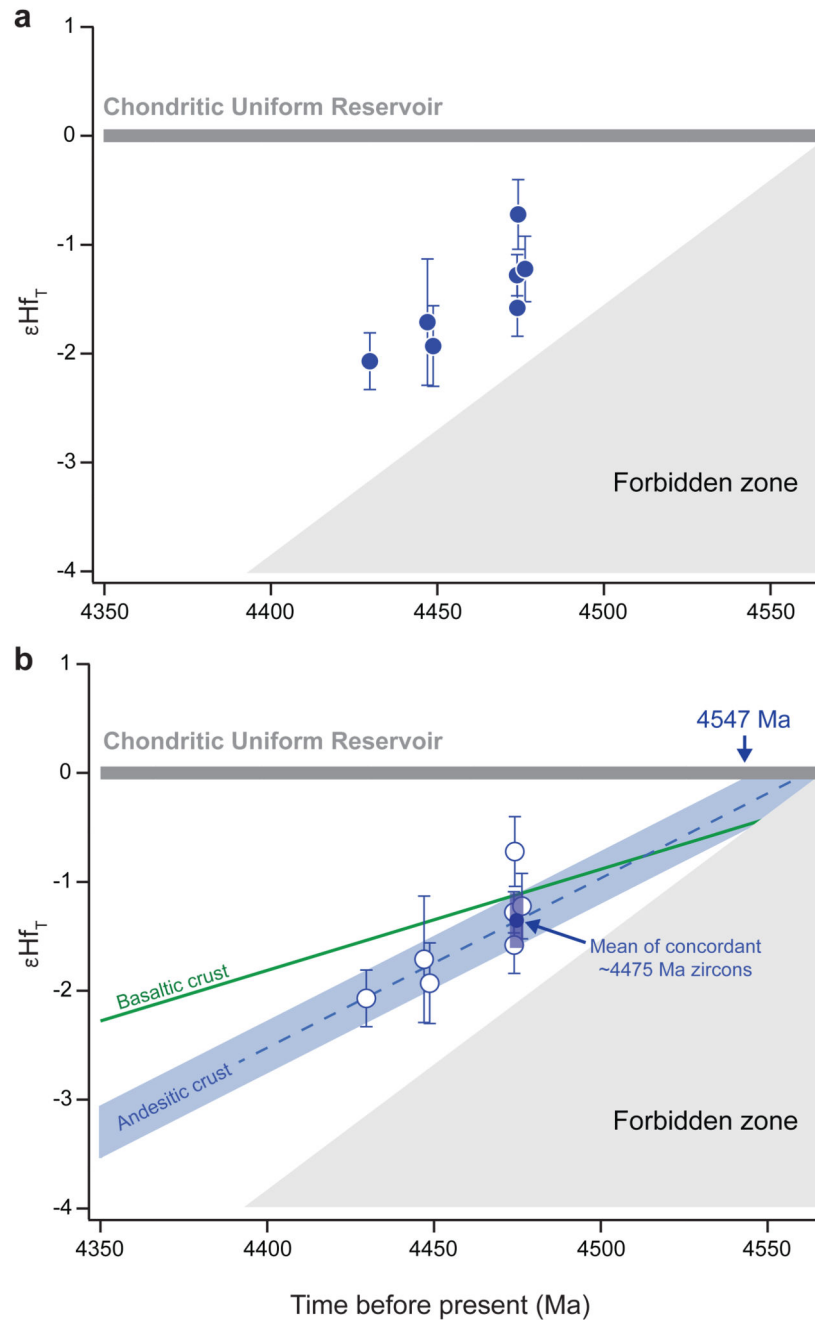


Fig. 2. Hf isotope evolution diagrams.

Shown in (A) are the initial ϵ_{Hf} values for the seven individual NWA 7034 zircons calculated with their corresponding ^{207}Pb - ^{206}Pb ages using a $\lambda^{176}\text{Lu}$ value of $1.867 \pm 0.008 \times 10^{-11} \text{ year}^{-1}$ (ref. 30) and Chondritic Uniform Reservoir parameters of ref. 18. The upper boundary of the forbidden region represents a reservoir with a $^{176}\text{Lu}/^{177}\text{Hf} = 0$ and a formation age defined by the age of the Solar System at 4567 Ma³¹. In (B), we show the time evolution of basaltic and andesitic crustal reservoirs required to account for the average initial Hf isotope compositions of the three concordant 4475 Ma zircons (S24b4,

S24b7 and S25b10) using $^{176}\text{Lu}/^{177}\text{Hf}$ ratios of 0.020 and 0.011 for the basaltic and andesitic crusts, respectively^{23,25}. Considering the upper uncertainty of the zircon average ϵHf value (-1.35 ± 0.22), it is not possible to account for the initial Hf isotope composition of these grains if they formed from the reworking of a basaltic crust since extraction ages older than the Solar System are required. In contrast, using a more evolved, andesite-like $^{176}\text{Lu}/^{177}\text{Hf}$ ratio returns a minimum extraction age of 4547 Ma. Using the mean of the concordant grains at face value and a $^{176}\text{Lu}/^{177}\text{Hf}$ ratios of 0.011 yields an extraction age of 4562^{+5}_{-15} Ma. Note that the time evolution of this reservoir can account for the Hf isotope composition of the younger ~4450 Ma and ~4430 Ma zircons. Indeed, a regression of the mean of the ~4475 Ma, ~4450 Ma and ~4430 Ma zircons yields a slope corresponding to an andesite-like $^{176}\text{Lu}/^{177}\text{Hf}$ ratio of 0.011. Uncertainty on the ϵHf values reflect the internal precision (2SE) or the external reproducibility of 22 ppm, whichever is larger. Uncertainty on the $^{207}\text{Pb}/^{206}\text{Pb}$ ages (2σ) are smaller than symbols.

Table 1
U-Pb age data and ^{176}Lu - ^{176}Hf systematics of NWA 7034 zircons and Hf isotope composition of the 91500 terrestrial zircon standard.

Age uncertainties are 2σ . Hf isotope ratios are reported normalized to the composition of the JMC-475 Hf standard. Uncertainties on the Hf isotope ratios reflect the 2SE internal precision in last decimal places. The external reproducibility of the $^{176}\text{Hf}/^{177}\text{Hf}$ ratio is estimated to be 22 ppm based on the analyses of the seven 91500 zircon aliquots. U-Pb data are reported in full in Table S1.

Sample	$^{207}\text{Pb}/^{206}\text{Pb}$ age (Ma)	$^{207}\text{Pb}/^{235}\text{U}$ age (Ma)	$^{206}\text{Pb}/^{238}\text{U}$ age (Ma)	$^{176}\text{Lu}/^{177}\text{Hf}$	$^{176}\text{Hf}/^{177}\text{Hf}$	$^{178}\text{Hf}/^{177}\text{Hf}$	$^{180}\text{Hf}/^{177}\text{Hf}$	ϵHf_T
S22b4	4448.7 \pm 1.8	4445.1 \pm 6.3	4437.3 \pm 22.1	0.000805	0.279891 \pm 10	1.46718 \pm 2	1.88666 \pm 6	-1.92 \pm 0.37
S22b5	4474.2 \pm 1.4	4457.8 \pm 5.7	4421.9 \pm 19.8	0.000799	0.279907 \pm 09	1.46719 \pm 2	1.88666 \pm 5	-0.71 \pm 0.32
S23b9	4447.0 \pm 1.5	4441.0 \pm 4.8	4427.7 \pm 16.5	0.000911	0.279908 \pm 16	1.46721 \pm 2	1.88669 \pm 6	-1.70 \pm 0.58
S24b2	4429.7 \pm 1.0	4355.2 \pm 4.3	4195.9 \pm 12.8	0.001057	0.279922 \pm 06	1.46719 \pm 2	1.88667 \pm 3	-2.06 \pm 0.26
S24b4	4474.0 \pm 0.8	4470.1 \pm 2.9	4461.4 \pm 9.9	0.001055	0.279906 \pm 06	1.46719 \pm 2	1.88667 \pm 3	-1.57 \pm 0.26
S24b7	4473.9 \pm 0.9	4476.8 \pm 2.8	4483.3 \pm 9.5	0.000742	0.279887 \pm 05	1.46720 \pm 1	1.88667 \pm 3	-1.27 \pm 0.19
S25b10	4476.3 \pm 0.9	4474.5 \pm 3.6	4470.6 \pm 12.5	0.001191	0.279926 \pm 07	1.46721 \pm 2	1.88669 \pm 4	-1.21 \pm 0.30
<i>Average</i>						1.46720\pm2	1.88667\pm3	
91500-1					0.282308 \pm 06	1.46721 \pm 1	1.88670 \pm 3	
91500-2					0.282314 \pm 11	1.46718 \pm 2	1.88674 \pm 4	
91500-3					0.282311 \pm 06	1.46718 \pm 2	1.88670 \pm 4	
91500-4					0.282311 \pm 05	1.46718 \pm 1	1.88668 \pm 2	
91500-5					0.282309 \pm 05	1.46719 \pm 1	1.88669 \pm 2	
91500-6					0.282309 \pm 06	1.46718 \pm 1	1.88664 \pm 2	
91500-7					0.282317 \pm 05	1.46718 \pm 1	1.88667 \pm 3	
<i>Average</i>					0.282311\pm06	1.46718\pm2	1.88669\pm6	